Supplementary Information:

Invariant natural killer T cells recognize lipid self-antigen induced by microbial danger signals

Patrick J. Brennan[1,5], Raju V.V. Tatituri[1,5], Manfred Brigl[1], Edy Y. Kim[1], Amit Tuli[1], Joseph P. Sanderson[2], Stephan D. Gadola[2], Fong-Fu Hsu[3], Gurdyal S. Besra[4] and Michael B. Brenner[1]

[1]Department of Medicine, Division of Rheumatology, Immunology and Allergy, Brigham and Women's Hospital, Harvard Medical School, Boston, MA 02115, USA. [2]Academic Unit of Clinical & Experimental Sciences, University of Southampton, Faculty of Medicine, Sir Henry Wellcome and "Hope" Laboratories, United Kingdom. [3]Division of Endocrinology, Metabolism and Lipid Research, Washington University, St. Louis, MO 63110, USA. [4]School of Biosciences, University of Birmingham, Birmingham B15 2TT, UK. [5]Both authors contributed equally to this work.

Supplementary Table 1. Glycosphingolipids eluted from CD1d on APC

LacCer	**Gal**β1-4**Glc**β1-**Cer**
Asialo-GM1	**Gal**β1-**GalNAc**β1-4**Gal**β1-4**Glc**β1-**Cer**
Asialo-GM2	**GalNAc**β1-4**Gal**β1-4**Glc**β1-**Cer**
GM1	**Gal**β1-**GalNAc**β1-4(**NeuNAc**α2-3)**Gal**β1-4**Glc**β1-**Cer**
GM2	**GalNAc**β1-4(**NeuNAc**α2-3)**Gal**β1-4**Glc**β1-**Cer**
GM3	(**NeuNAc**α2-3)**Gal**β1-4**Glc**β1-**Cer**
GD1a	(**NeuNAc**α2-3)**Gal**β1-3**GalNAc**β1-4(**NeuNAc**α2-3)**Gal**β1-4**Glc**β1-**Cer**
GB3	**Gal**α1-4**Gal**β1-4**Glc**β1-**Cer**

Glc - glucose, Gal - galactose, Cer - ceramide, GalNAc - N-acetylglucosamine
NeuNAc - N-acetyl neuraminic acid

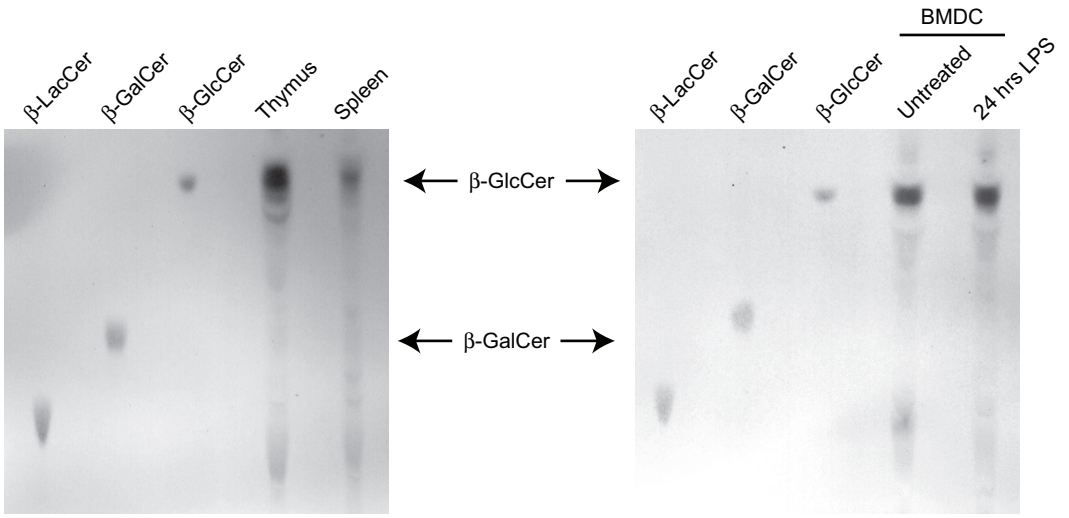

Supplementary Figure 1
β-GlcCer is the major monohexosyl ceramide of thymyus, spleen, and BMDC.
Borate-impregnated TLC was utilized to assess the relative contribution of β-GlcCer and β-GalCer species to the monohexosyl ceramide fraction from lymphoid tissues. Polar lipid extracts from the indicated organs were alkali-treated to remove glycerol-based lipids, allowing for visualization of both β-GlcCer and β-GalCer bands. The left panel shows lipid extracts from mouse thymus and spleen. The right panel shows lipid extracts from $CD11c^+$ BMDC cultured for 24 hrs in the presence or absence of 1 ng/ml LPS.

a

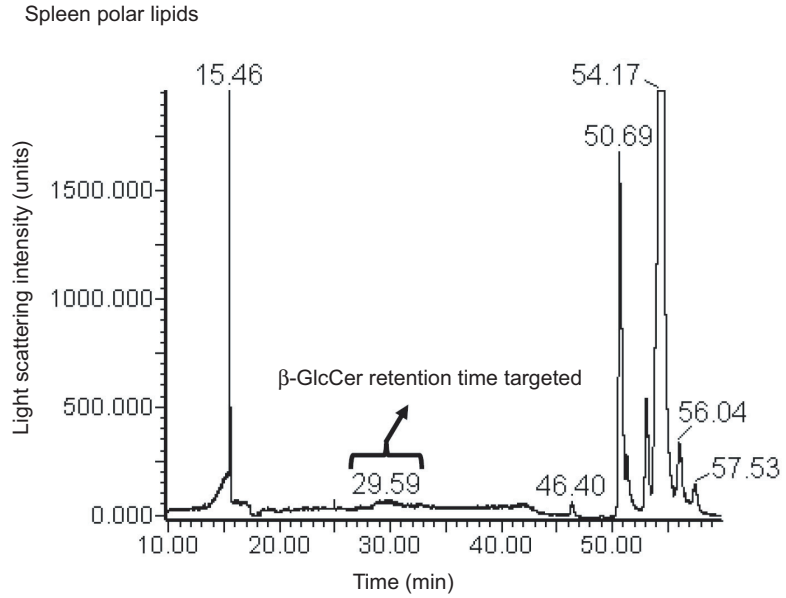

b

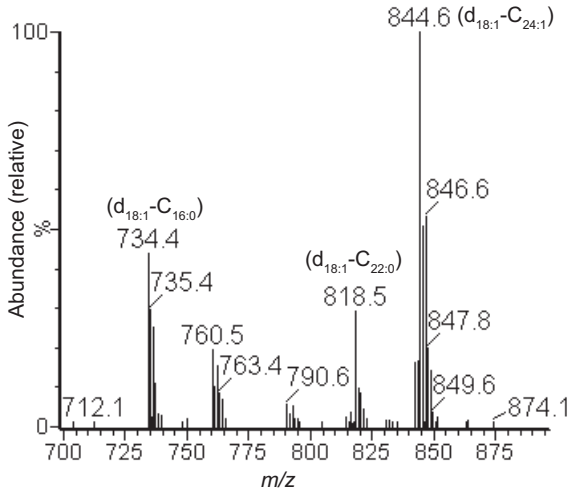

c

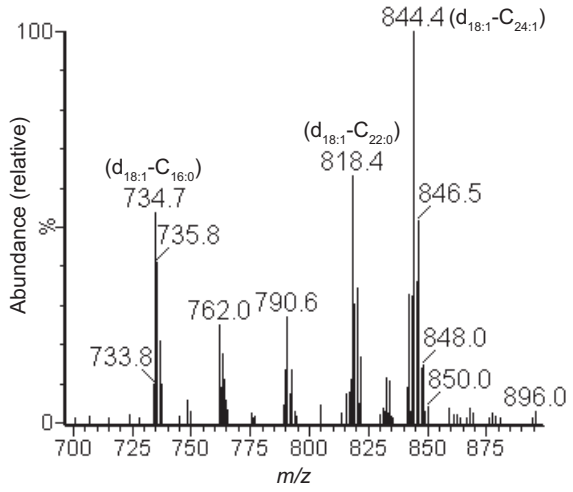

Supplementary Figure 2
Preparative HPLC enrichment of β-GlcCer from primary mouse tissues.
Polar lipid tissue extracts were subjected to preparative scale ternary-solvent gradient, normal-phase HPLC to separate lipids based on the polar head group, and collected using an automated fraction collector. **(a)** An example preparative separation of spleen polar lipid extract is shown. The β-GlcCer fraction was targeted by retention time of standards, and confirmed by real-time mass spectrometry. β-GlcCer fractions collected as above from mouse **(b)** thymus and **(c)** spleen total polar lipids were analyzed by MS, and mass spectra are shown with a chloride adduct in electrospray-negative mode. The predicted *N*-acyl chains based on the mass / charge ratio are shown in parentheses above the major peaks.

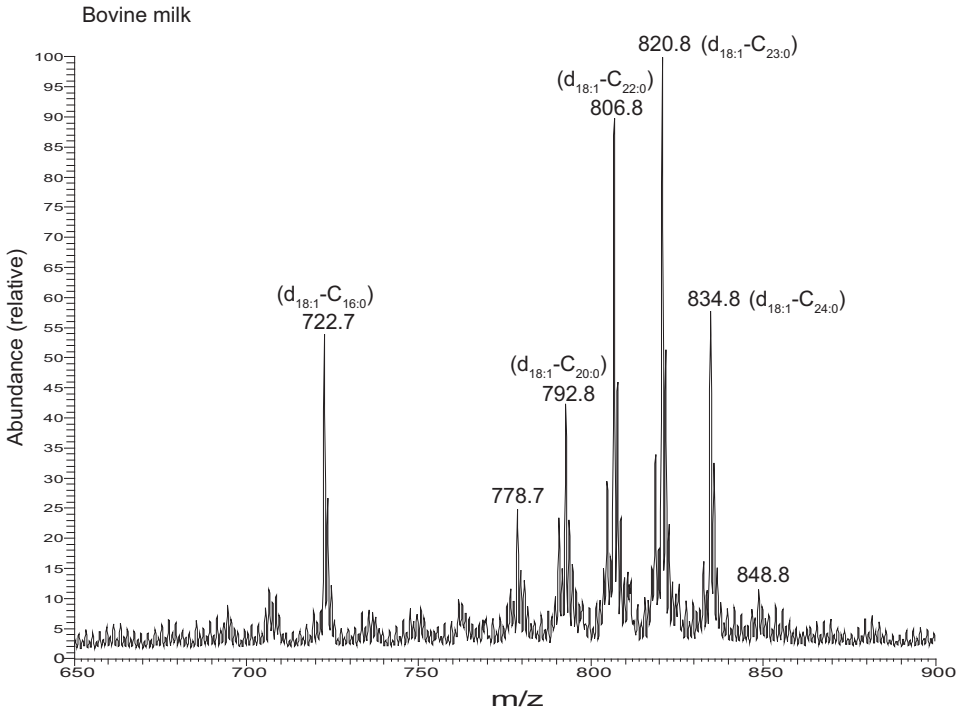

Supplementary Figure 3
Fatty acid composition of milk β-GlcCer.
Purified milk β-GlcCer was analyzed by ESI-MS, and results are depicted in electrospray-positive mode. Ions are shown with sodium adducts. Fatty acid composition as determined by CID-MS is shown in parentheses for major ions.

β-GlcCer ($d_{18:1}$-$C_{8:0}$)

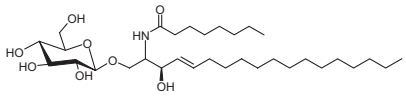

β-GlcCer ($d_{18:1}$-$C_{12:0}$)

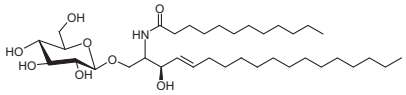

β-GlcCer ($d_{18:1}$-$C_{16:0}$)

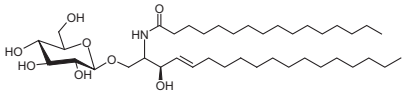

β-GlcCer ($d_{18:1}$-$C_{18:0}$)

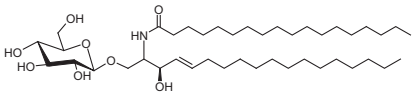

β-GlcCer ($d_{18:1}$-$C_{18:1}$)

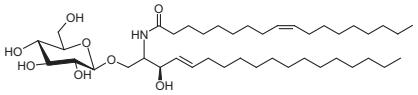

β-GlcCer ($d_{18:1}$-$C_{24:1}$)

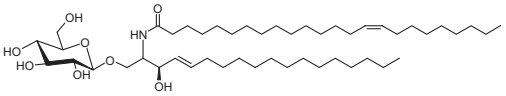

α-GalCer

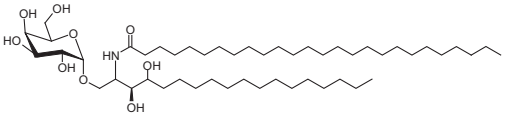

Supplementary Figure 4
Structures of the β-GlcCer compounds used in these studies are depicted along with that of α-GalCer.

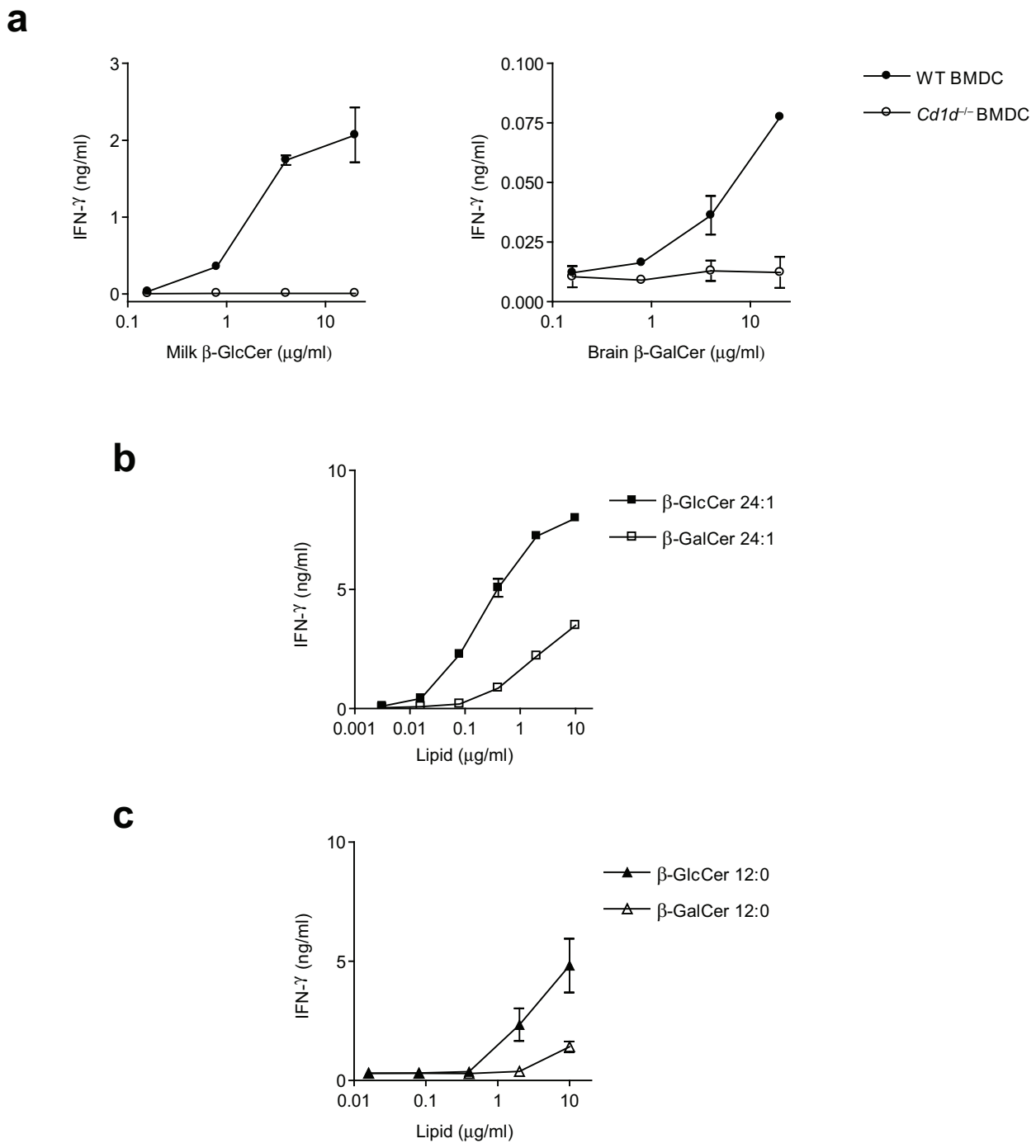

Supplementary Figure 5
β-GalCer activates iNKT cells.
A primary mouse iNKT cell line was co-cultured with either wild-type or CD1d-deficient $CD11c^+$ BMDC in the presence of the indicated β-GlcCer or β-GalCer species**. (a)** Bovine milk β-GlcCer (left panel) or brain β-GalCer (right panel) were compared. Note the y-axis scale difference. Synthetic β-GlcCer and β-GalCer with **(b)** $d_{18:1}$-$C_{24:1}$ and **(c)** $d_{18:1}$-$C_{12:0}$ fatty acid composition were also compared. ELISA data are presented as mean and range in duplicate wells, and are representative of three separate experiments.

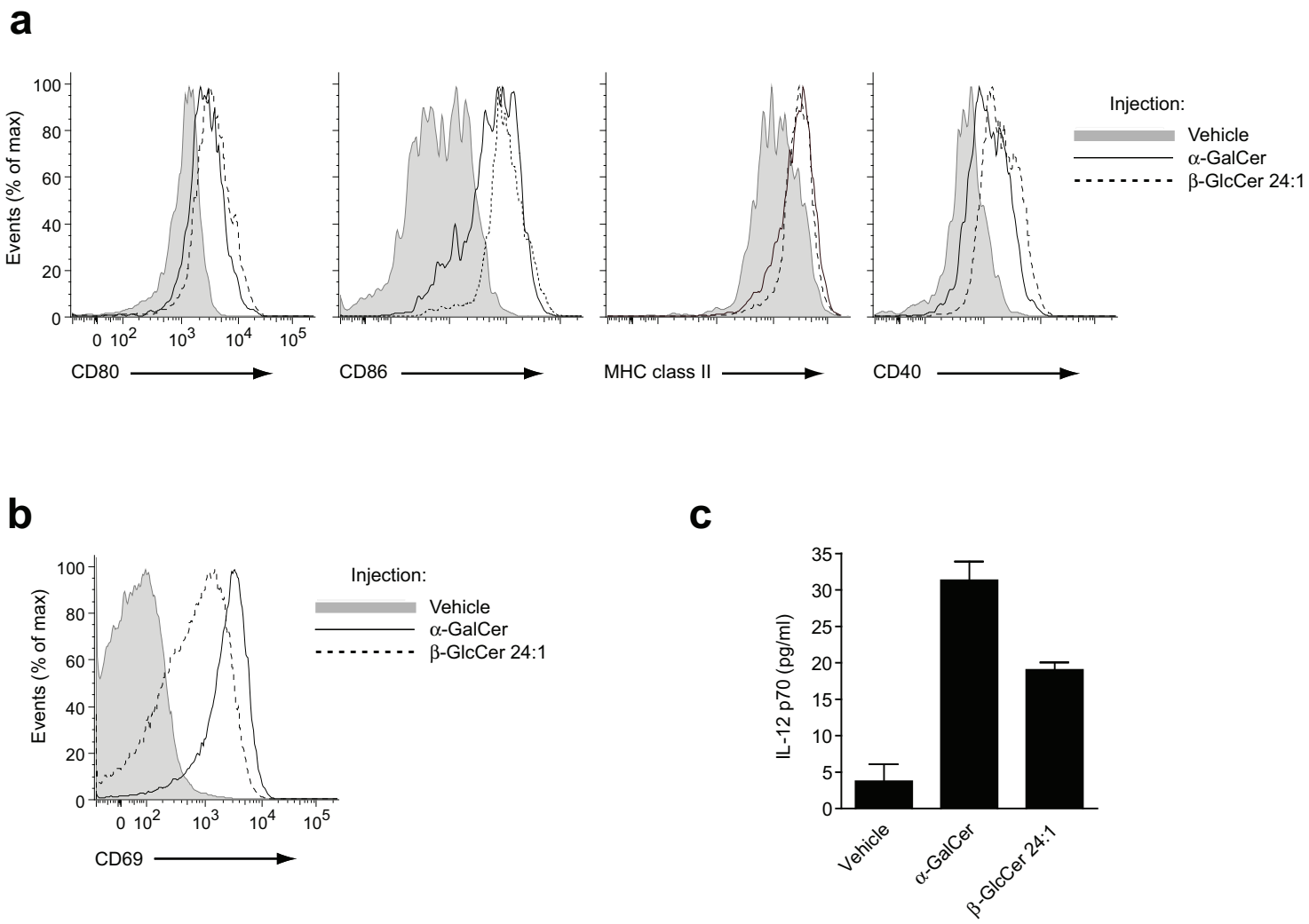

Supplementary Figure 6
Activation of CD11c$^+$ dendritic cells and B cells following β-GlcCer exposure *in vivo*.
Wild-type C57Bl/6 mice were injected intravenously with vehicle, α-GalCer (1 μg), or β-GlcCer 24:1 (25 μg) and spleens were harvested after 24 hrs. **(a)** The expression of activation markers CD80, CD86, MHC class II, and CD40 in spleen dendritic cells following intravenous injection of lipid was assessed by flow cytometry, with the CD11c$^+$CD19$^-$CD3ε$^-$ gate shown. **(b)** B cell activation was assessed by CD69 upregulation, with the CD19$^+$CD3ε$^-$ lymphocyte gate shown. **(c)** Serum IL-12 following lipid injection was assessed by IL-12 p70 ELISA, with data presented as mean and range in duplicate wells. Data are representative of two separate experiments with two mice per group.

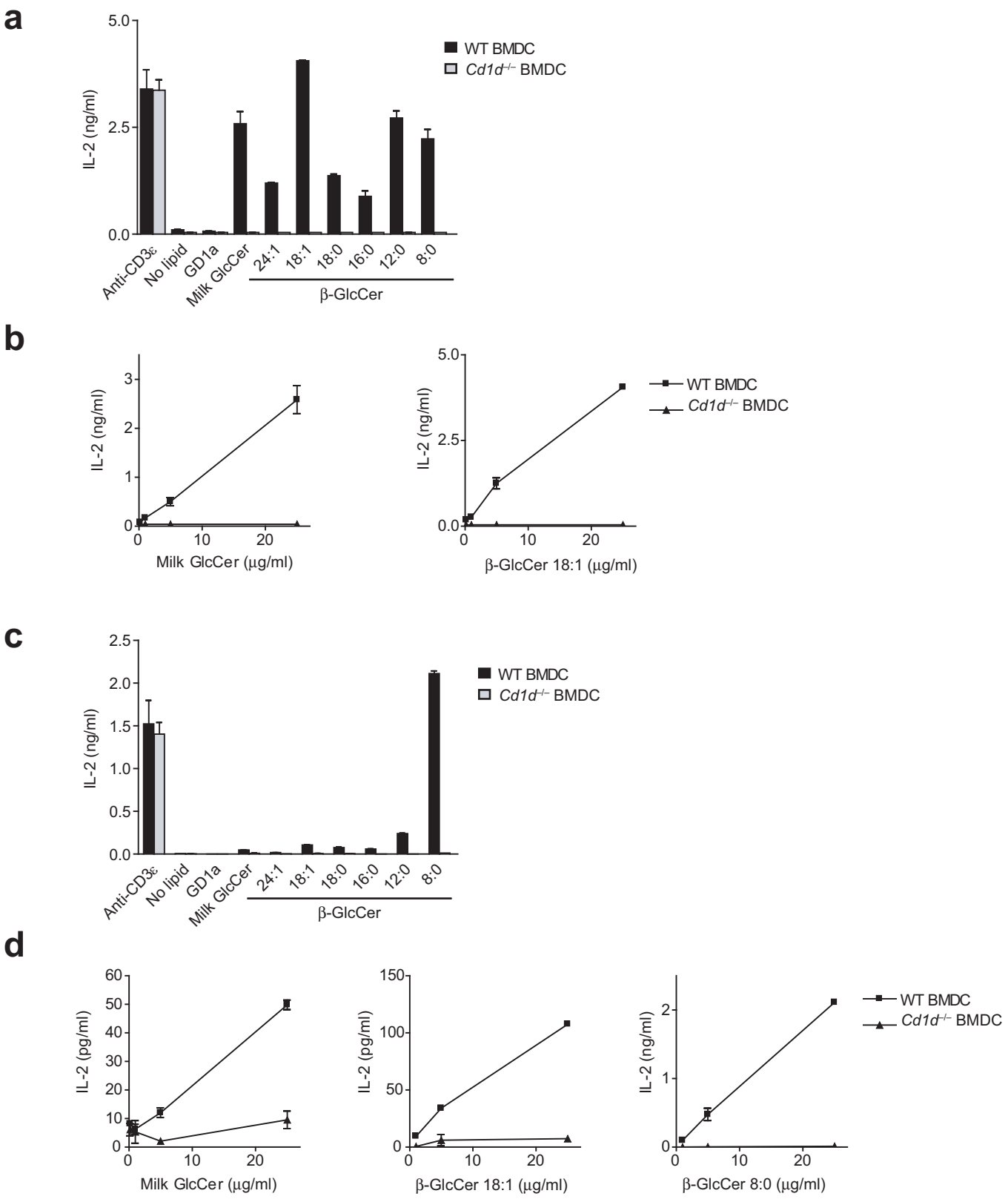

Supplementary Figure 7

β-GlcCer activates NKT cell hybridomas bearing diverse TCRs.

The diverse NKT hybridomas **(a)** VII68 and **(c)** XV19 were co-cultured with $CD11c^+$ BMDC in the presence of the 25 μg/ml of the indicated lipid or 10 ng/ml anti-CD3ε. For selected lipids, a dose titration is shown for **(b)** VII68 and **(d)** XV19. Note y-axis scale differences. ELISA data are presented as mean and range in duplicate wells, and are representative of three separate experiments.

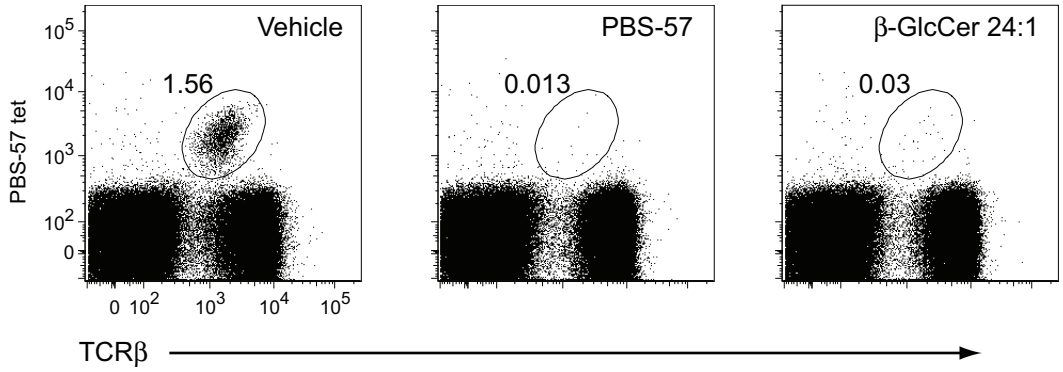

Supplementary Figure 8
β-GlcCer 24:1 leads to iNKT TCR downregulation *in vivo*.
Wild-type C57Bl/6 mice were injected intravenously as in Supplementary Fig. 6, and spleens were harvested after 24 hrs. The iNKT cell population was assessed by staining with TCRβ antibody and PBS-57-loaded CD1d tetramer, with the $CD19^-$ lymphocyte gate shown. Results are representative of two experiments.

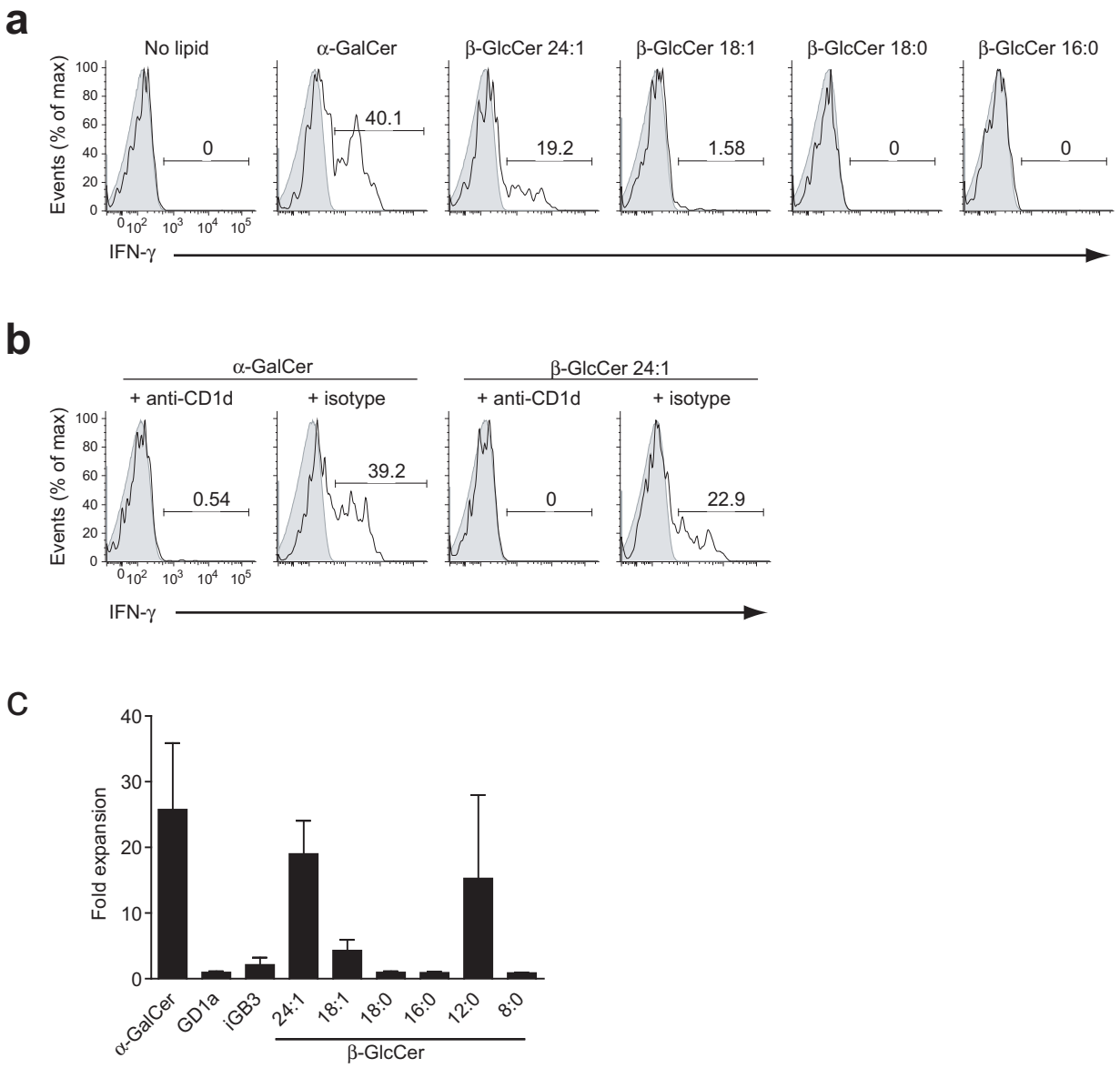

Supplementary Figure 9
β-GlcCer activity on human iNKT cells.
(a) Intracellular cytokine staining of iNKT cells from freshly-isolated PBMC following culture with 25 μg/ml of the indicated lipid, or 1 μg/ml of α-GalCer and **(b)** in the presence of a CD1d-blocking (42.1) or isotype control monoclonal antibody, with the $CD3\varepsilon^+$PBS-57 $tetramer^+$ gate shown for all plots. Data are representative of three separate experiments. **(c)** For five healthy donors, freshly-isolated PBMC were cultured with 1 μg/ml of the indicated lipid for 8 days, and analyzed by flow cytometry after staining with $CD3\varepsilon^+$ and PBS-57 tetramer. Fold expansion in the $CD3\varepsilon^+$ / PBS-57 $tetramer^+$ gate relative to the total $CD3\varepsilon^+$ population is shown. Error is presented as s.e.m. among donors.

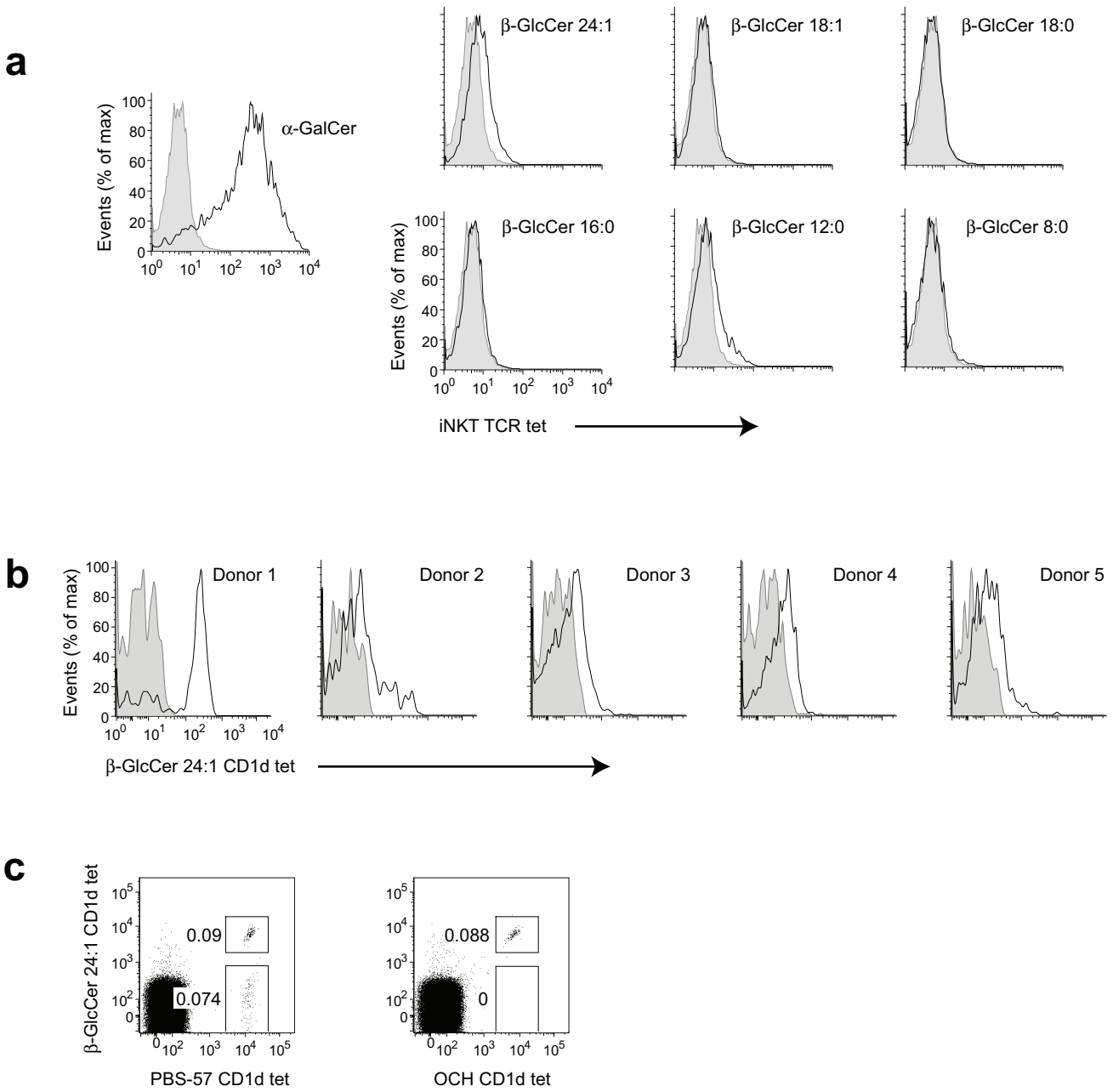

Supplementary Figure 10

β-GlcCer-loaded CD1d and iNKT cell TCR tetramers demonstrate a cognate TCR-lipid-CD1d interaction in human.

(a) A T2 lymphoblast cell line transfected with CD1d was pulsed with the indicated lipids for 3 hrs, washed, and the binding of a phycoerythrin-conjugated iNKT TCR tetramer was assessed by flow cytometry. Filled tracings represent iNKT TCR tetramer binding to vehicle-pulsed T2 cells. Results are representative of three independent experiments. **(b)** β-GlcCer $C_{24:1}$ -loaded CD1d tetramer binding overlaid on unloaded tetramer (filled tracing) is shown for iNKT cells from five healthy donors, with the $CD3\varepsilon^+$/PBS-57-loaded CD1d $tetramer^+$ gate shown. **(c)** PBMC co-stained with β-GlcCer $C_{24:1}$ CD1d tetramer and PBS-57 or OCH-loaded CD1d tetramers, with the $CD3\varepsilon^+$ gate shown. Results are representative of two experiments.

a

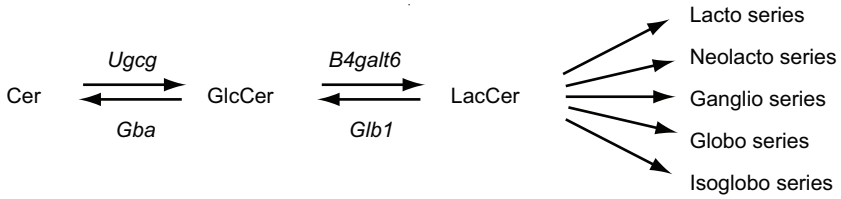

b

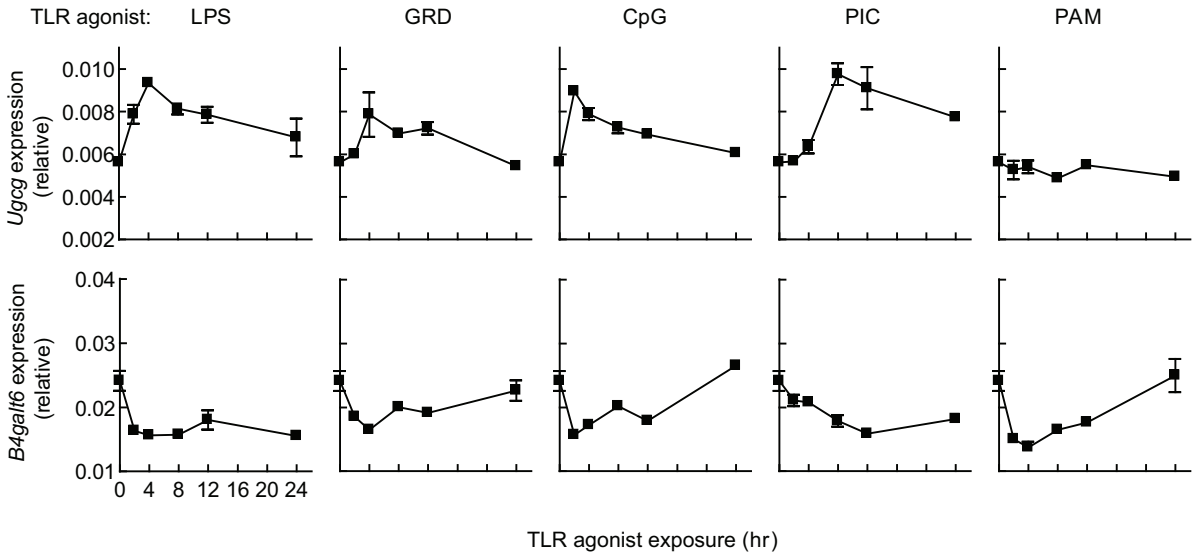

Supplementary Figure 11
Gene expression analysis in BMDC following TLR agonist exposure.
(a) The genes involved in β-GlcCer metabolism are depicted. **(b)** Murine CD11c^{+} expression profiling data following TLR agonist exposure, generated by Amit *et al*., *Science* (2009), was analyzed for *Ugcg* and *B4galt6* expression, shown relative to *Gapdh*. TLR agonist abbreviations with the major TLR activated: Lipopolysaccharide (LPS, TLR4), Gardiquimod (GRD, TLR7) , CpG (TLR9), Poly(I:C) (PIC, TLR3), PAM3CSK (PAM, TLR2).

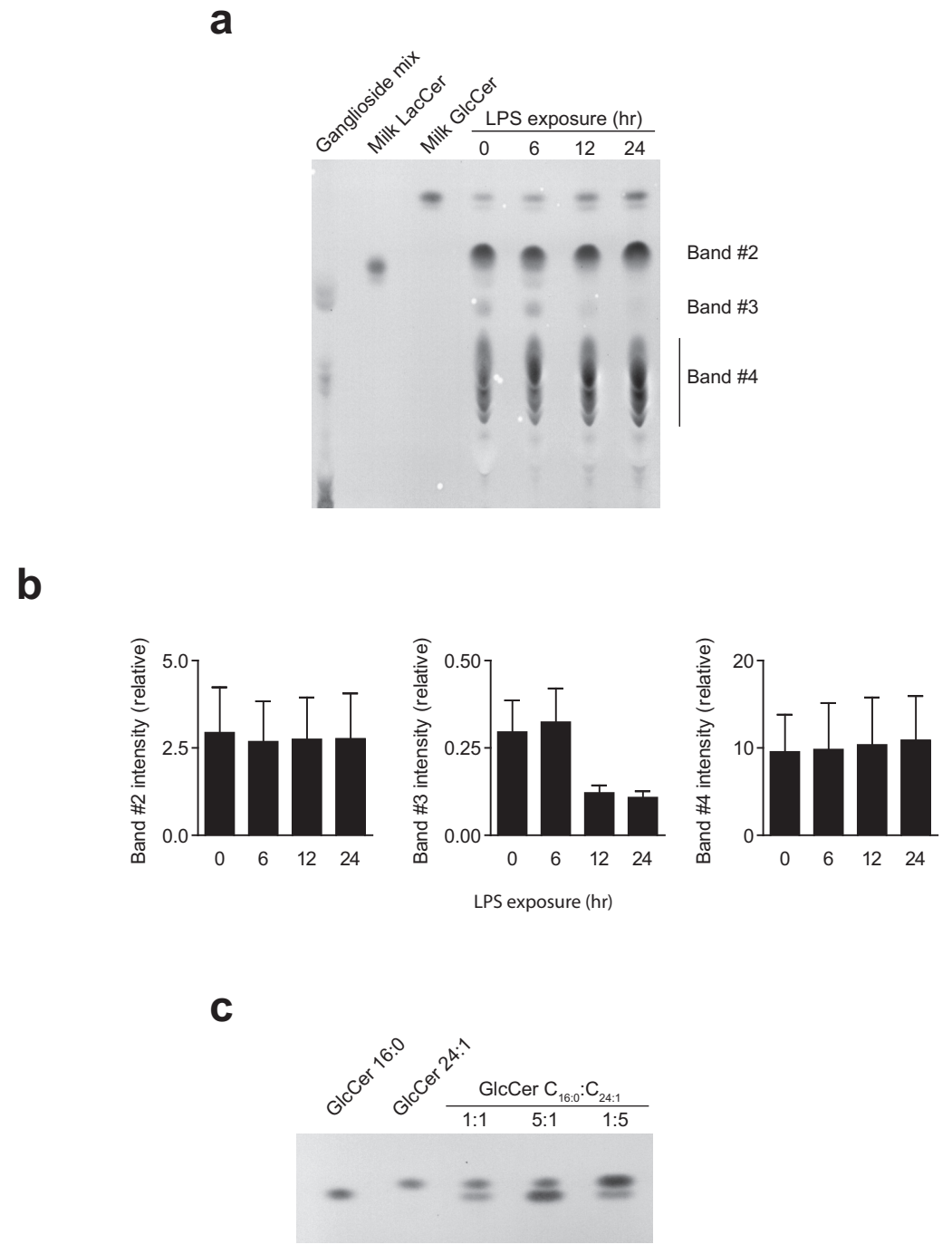

Supplementary Figure 12
TLC analysis of CD11c$^+$ BMDC.
(a) TLC analysis of polar lipid extracts from LPS-treated CD11c$^+$ BMDC with query bands indicated. **(b)** Densitometric quantification of the indicated bands relative to a milk β-GlcCer standard, with error reported as s.d. of relative band intensity. **(c)** TLC analysis of β-GlcCer $C_{16:0}$ and β-GlcCer $C_{24:1}$ loaded in the indicated ratios. Two independent experiments were performed, and a representative experiment is shown.

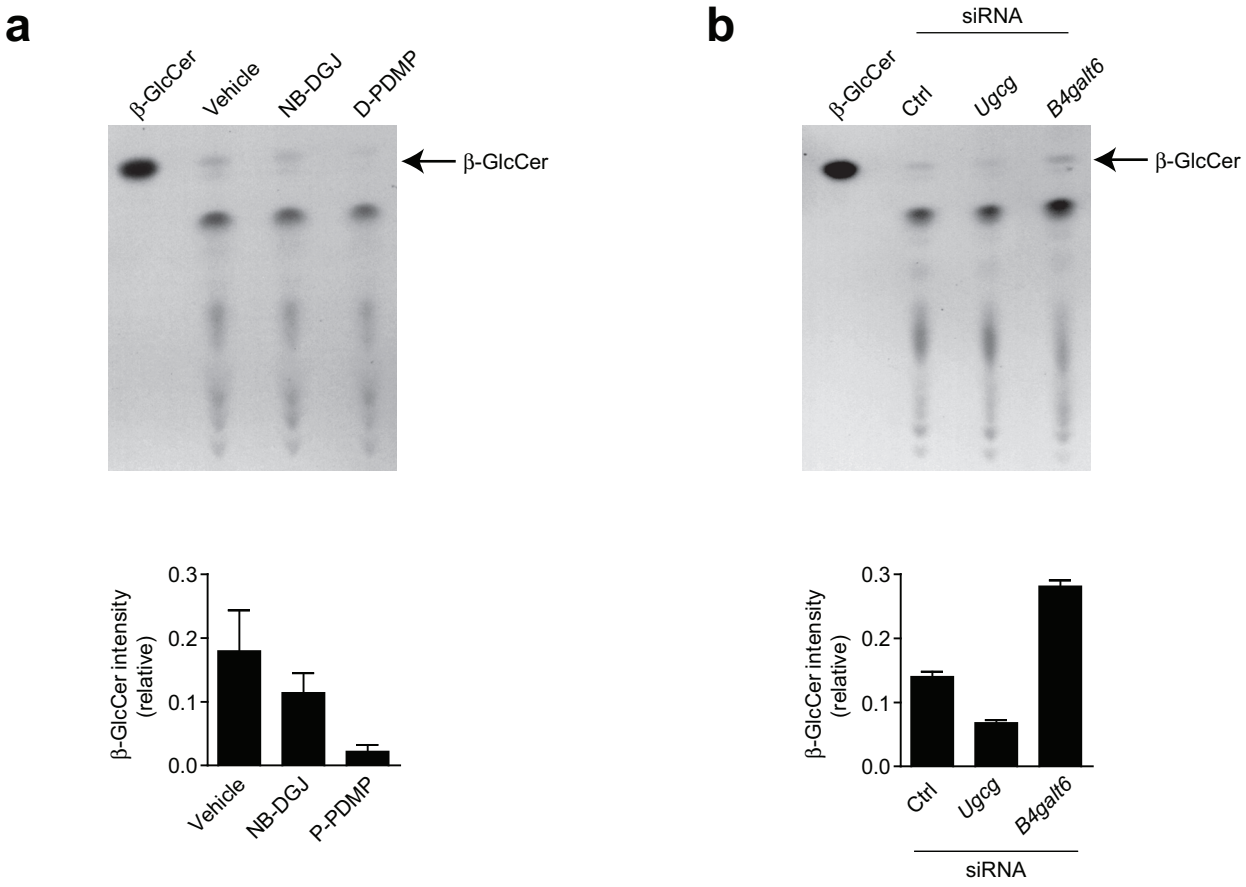

Supplementary Figure 13
TLC analysis of β-GlcCer synthesis inhibitor-treated and siRNA-silenced CD11c$^+$ BMDC.
(a) CD11c$^+$ BMDC were treated for 24 hrs with 1 ng/ml LPS in the presence of vehicle (methanol), NB-DGJ, or D-PDMP. **(b)** The indicated siRNA was introduced into CD11c$^+$ BMDC, and after 24 hrs, 1 ng/ml LPS was added to the culture for an additional 24 hrs. TLC analysis of polar lipid extracts is shown. Densitometric quantification is shown for each experiment, with error reported as s.d. of relative band intensity. Two independent experiments were performed, and a representative experiment is shown.

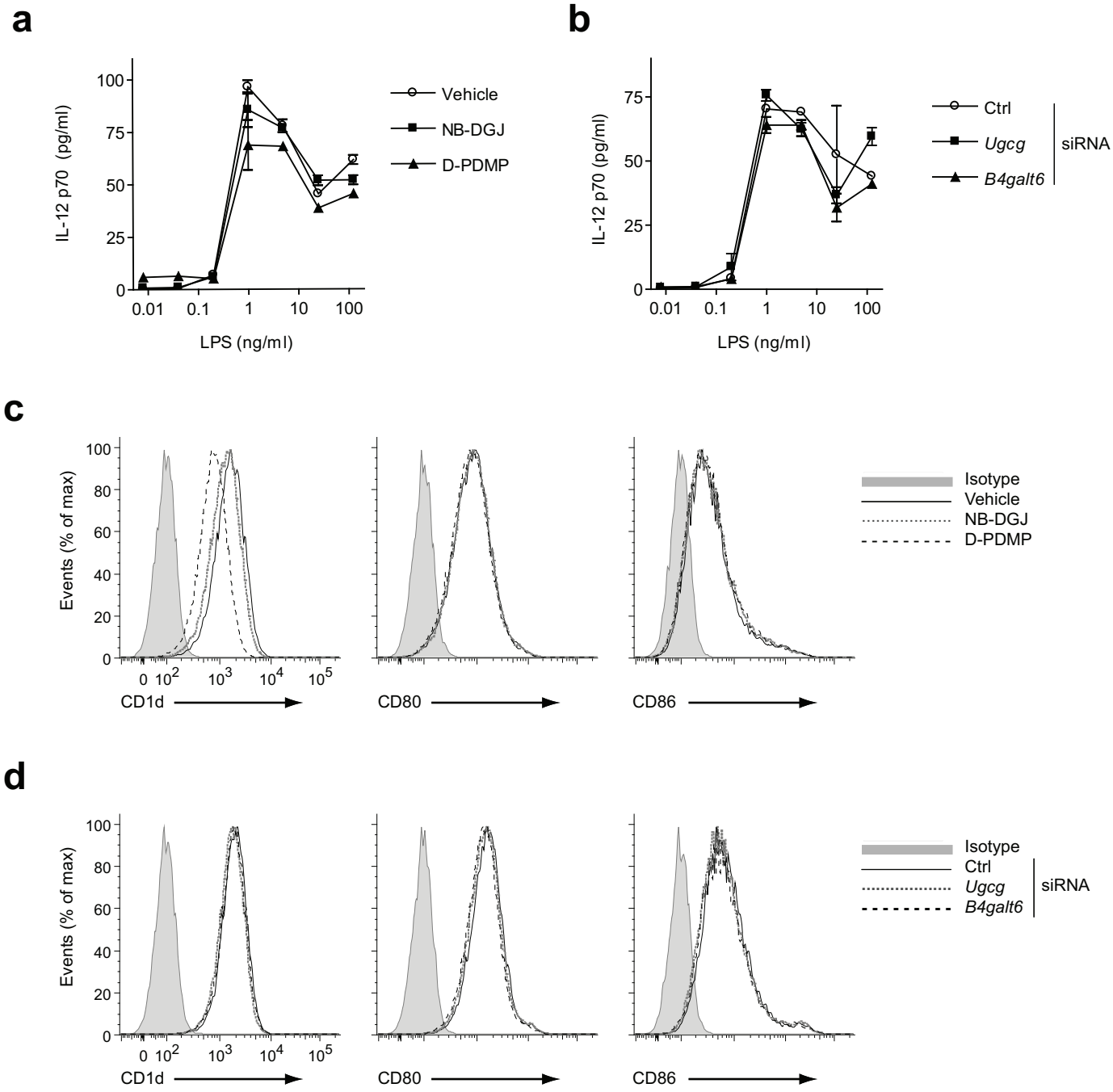

Supplementary Figure 14
Analysis of IL-12 production and BMDC activation marker expression following β-GlcCer synthesis inhibitor treatment and siRNA silencing.
$CD11c^+$ BMDC **(a)** in the presence of the indicated β-GlcCer synthesis inhibitor, or **(b)** silenced with the indicated siRNA, were co-cultured with a primary iNKT cell line in the presence of 1 ng/ml LPS, and IL-12 p70 was measured by ELISA. **(c)** $CD11c^+$ BMDC were treated for 24 hrs with 1 ng/ml LPS in the presence of vehicle (methanol) NB-DGJ, or D-PDMP, and flow-cytometric analysis of activation markers was performed. **(d)** The indicated siRNA was introduced into $CD11c^+$ BMDC, and after 24 hrs, 1 ng/ml LPS was added to the culture for an additional 24 hrs, followed by flow-cytometric analysis. Data are representative of two independent experiments.

a

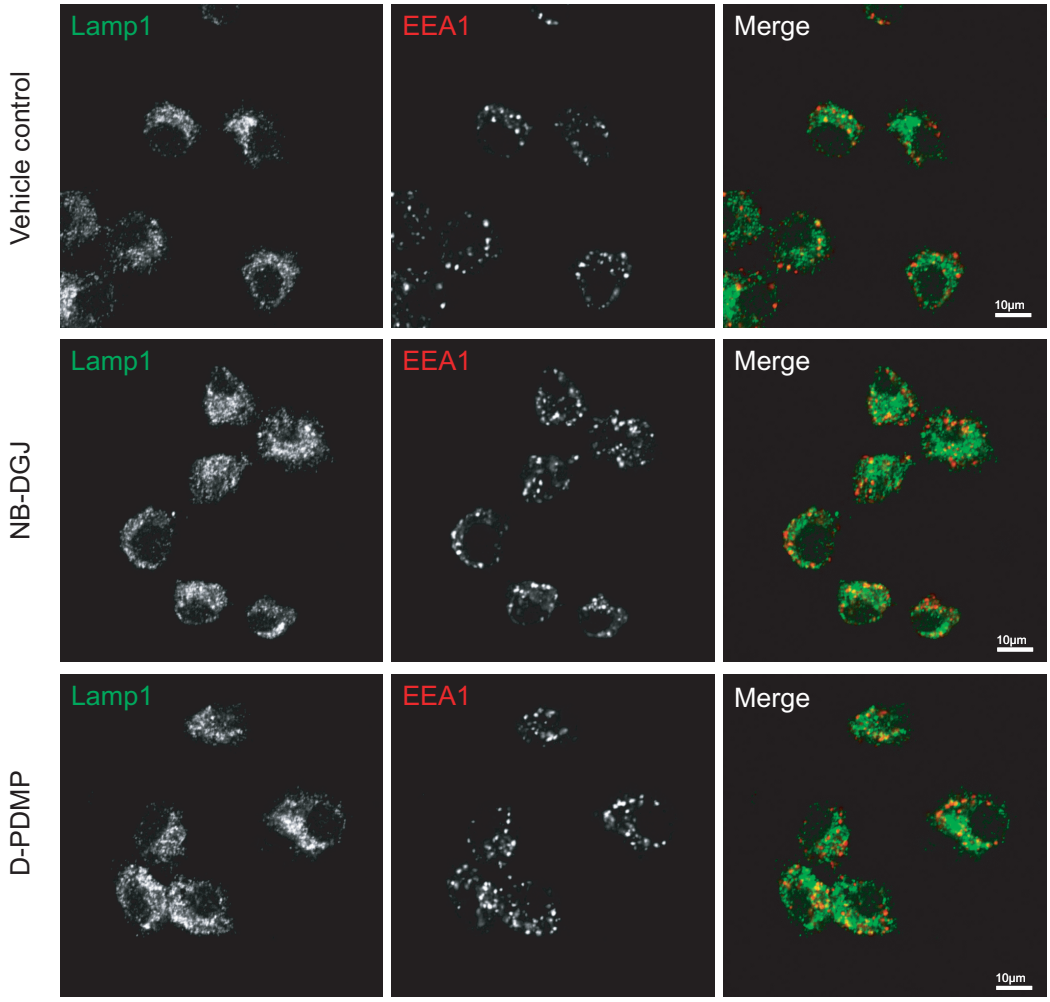

Supplementary Figure 15
Morphological analysis of CD11c^{+} BMDC following β-GlcCer synthesis inhibitor treatment and siRNA silencing.
(a) CD11c^{+} BMDC were analyzed by confocal microscopy in the presence of vehicle or the indicated β-GlcCer synthesis inhibitor, or **(b)** after introduction of the indicated siRNA. Analysis of endosomal and lysosomal compartments following 24 hrs of exposure to 1 ng/ml LPS was performed using antibodies against EEA-1 and LAMP-1. Data are representative of two independent experiments.

b

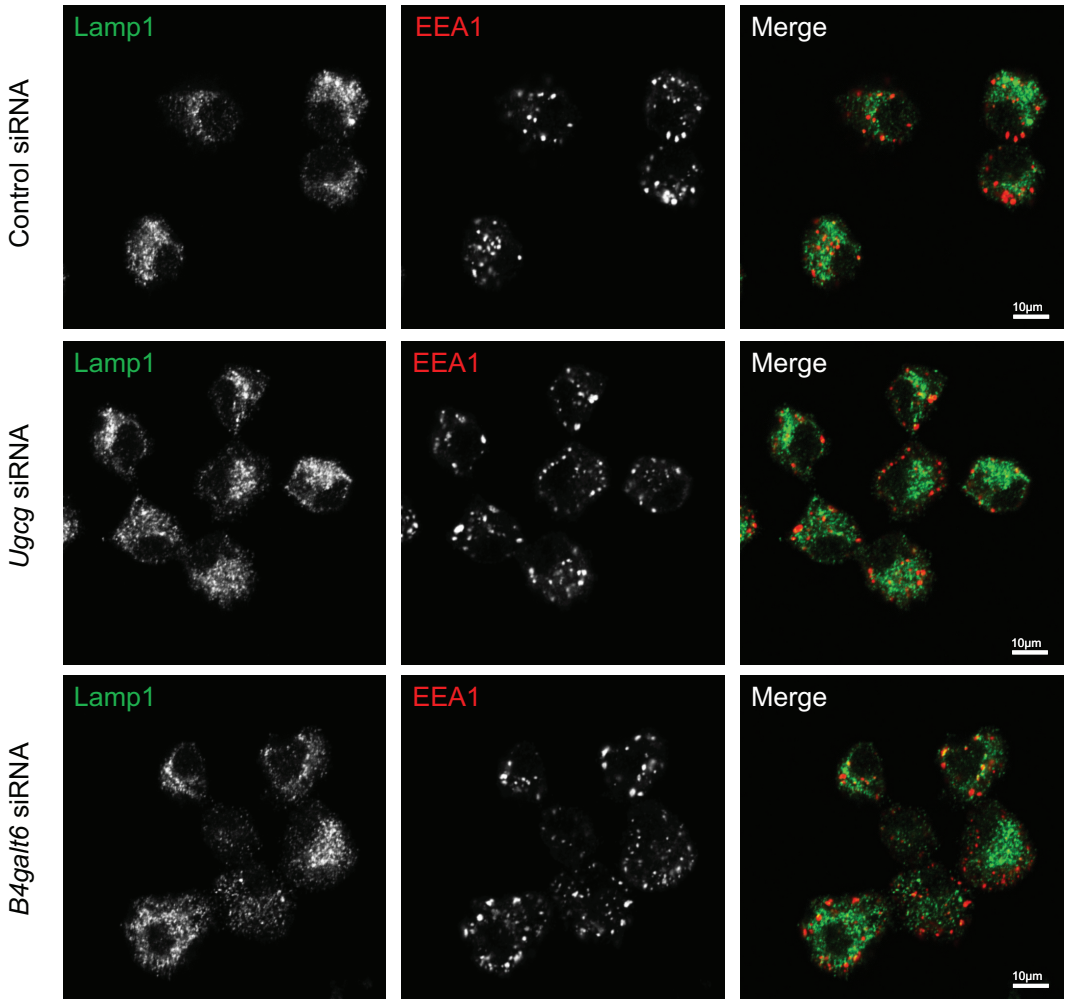

Supplementary Figure 15
Morphological analysis of CD11c^{+} BMDC following β-GlcCer synthesis inhibitor treatment and siRNA silencing.

Supplementary Methods

TLC and preparative HPLC analyses.

Borate-impregnated TLC plates were prepared by soaking silica plates in 2.5% boric acid (Sigma-Aldrich) in CH_3OH followed by activation at 110 ºC, and run in 65:35:4:4; $CHCl_3$:CH_3OH:25% NH_4OH: H_2O (v/v/v/v) prior to visualization[1]. Samples for analysis on borate-impregnated TLC were alkali-treated in methanolic KOH for 1 hr at 80 ºC, followed by neutralization, desalting, and re-extraction of polar lipids. Normal-phase preparative HPLC was performed using a Waters AutoPurification HPLC system coupled to mass spctrometry, evaporative light scattering, and photodiode array detectors.

Dendritic cell, B cell, and IL-12 evaluation.

For evaluation of B cell and $CD11c^+$ dendritic cell activation, spleens were harvested 24 hrs after lipid injection and used for flow cytometric analysis. Antibodies against CD80(16-10A1), CD86(GL1), I-A/I-E (M5.114.15.2), CD40 (3/23), CD69 (H1.2F3) and CD19 (1D3) were from BD biosciences. For serum IL-12 analysis following injection of lipids, blood was harvested by cardiac puncture and serum obtained using serum separator tubes (BD Biosciences). Anti-mouse IL-12 p70 antibodies for ELISA were from eBioscience.

Diverse iNKT cell hybridomas.

The following diverse NKT cell hybridomas were tested: 14s.6, 14s.7, 14s.10, 14s.15, TB.A7, TC.B11, 431.A11, VIII24, VII68, XV19[2-4]. Those not generated in our laboratory were kindly provided by S. Cardell and A. Bendelac. For assay, 5 x 10^4 diverse iNKT cells were co-cultured with 10^4 $CD11c^+$ BMDC per well.

Human intracellular cytokine staining.

For human intracellular cytokine staining, 25 μg of each lipid or 1 μg α-GalCer was added to 2 x 10^6 PBMC in 1 ml of culture media for 12 hrs. Monensin (BD Biosciences) was added to the culture for an additional 4 hrs. Staining was performed using the BD Biosciences cytofix/cytoperm kit according to the manufacturer's instructions. Anti-IFN-γ (4S.B3) was from eBioscience.

Human iNKT cell TCR tetramer analysis.

The human CD1d-transfected T2 lymphoblast cell line and the generation of human iNKT TCR tetramers have been previously described[5]. Prior to tetramer binding, the CD1d-transfected lymphoblast cell line was pulsed with 10 μg/ml of the indicated lipid in RPMI with 0.05% Tween-20 for 3 hrs at 37 ºC.

Human iNKT cell expansion.

PBMC were freshly isolated by density centrifugation over Ficoll, and 1 x 10^6 PBMC in 2 ml culture media supplemented with 50 U/ml IL-2 (Novartis) and 5 ng/ml IL-15 (Peprotech), were incubated for 8 days in the presence of 1 μg/ml lipid prior to analysis.

Gene expression data analysis.
Mouse BMDC expression data was downloaded from the NIH geo database, accession number GSE17721[6]. RMA normalized sample probe intensity is expressed relative to *Gapdh* for consistency with qPCR data analysis. Error is reported as s.e.m. among duplicate samples and probes.

qPCR primer sequences:
Gapdh forward primer: 5'-GTCGTGGATCTGACGTGCC-3'
Gapdh reverse primer: 5'-GATGCCTGCTTCACCACCTT-3'
Ugcg forward primer: 5'-TGCATGCTACACTTTCCTCTCCGT-3'
Ugcg reverse primer: 5'-AGCATCAGATGGATAACACGCCCT-3'
B4galt6 forward primer: 5'-TATGTCATCGAACAGACCGGCACA-3'
B4galt6 reverse primer: 5'-AGGCTCTGTCTTTCATGGCCTCTT-3'
Gba forward primer: 5'-TTCACCAGACCTGGGCCAATTACT-3'
Gba reverse primer: 5'-TGCTGTAGGTTCATTCTCCGCTGT-3'
Glb1 forward primer: 5'-TCAAGGATGGACAGCCATTCCGAT-3'
Glb1 reverse primer: 5'-TCAGCCCAGCCATCTTCATCTTCA-3'

Confocal microscopy.
$CD11c^+$ BMDC were adhered to coverslips coated with poly-L lysine (Sigma-Aldrich) and fixed with 4% paraformaldehyde. Permeabilization and antibody staining was done with 0.5% BSA, 0.2% Saponin in PBS. Anti-LAMP1 antibody was from BD Transduction Laboratories, and anti-EEA1 was from Calbiochem. Images were obtained with a Nikon TE2000-U inverted confocal microscope.

1. Kean, E.L. Separation of gluco- and galactocerebrosides by means of borate thin-layer chromatography. *J Lipid Res* **7**, 449-452 (1966).
2. Behar, S.M., Podrebarac, T.A., Roy, C.J., Wang, C.R. & Brenner, M.B. Diverse TCRs recognize murine CD1. *J Immunol* **162**, 161-167 (1999).
3. Cardell, S. *et al.* CD1-restricted CD4+ T cells in major histocompatibility complex class II-deficient mice. *J Exp Med* **182**, 993-1004 (1995).
4. Park, S.H., Roark, J.H. & Bendelac, A. Tissue-specific recognition of mouse CD1 molecules. *J Immunol* **160**, 3128-3134 (1998).
5. Matulis, G. *et al.* Innate-like control of human iNKT cell autoreactivity via the hypervariable CDR3beta loop. *PLoS Biol* **8**, e1000402 (2010).
6. Amit, I. *et al.* Unbiased reconstruction of a mammalian transcriptional network mediating pathogen responses. *Science* **326**, 257-263 (2009).